



This is a repository copy of *Correlating three-dimensional morphology with function in PBDB-T:IT-M non-fullerene organic solar cells*.

White Rose Research Online URL for this paper:
<http://eprints.whiterose.ac.uk/156040/>

Version: Supplemental Material

Article:

Li, W., Cai, J., Yan, Y. et al. (11 more authors) (2018) Correlating three-dimensional morphology with function in PBDB-T:IT-M non-fullerene organic solar cells. *Solar RRL*, 2 (9). 1800114. ISSN 2367-198X

<https://doi.org/10.1002/solr.201800114>

This is the peer reviewed version of the following article: Li, W., Cai, J., Yan, Y., Cai, F., Li, S., Gurney, R.S., Liu, D., McGettrick, J.D., Watson, T.M., Li, Z., Pearson, A.J., Lidzey, D.G., Hou, J. and Wang, T. (2018), Correlating Three-dimensional Morphology With Function in PBDB-T:IT-M Non-Fullerene Organic Solar Cells. *Sol. RRL*, 2: 1800114, which has been published in final form at <https://doi.org/10.1002/solr.201800114>. This article may be used for non-commercial purposes in accordance with Wiley Terms and Conditions for Use of Self-Archived Versions.

Reuse

Items deposited in White Rose Research Online are protected by copyright, with all rights reserved unless indicated otherwise. They may be downloaded and/or printed for private study, or other acts as permitted by national copyright laws. The publisher or other rights holders may allow further reproduction and re-use of the full text version. This is indicated by the licence information on the White Rose Research Online record for the item.

Takedown

If you consider content in White Rose Research Online to be in breach of UK law, please notify us by emailing eprints@whiterose.ac.uk including the URL of the record and the reason for the withdrawal request.



eprints@whiterose.ac.uk
<https://eprints.whiterose.ac.uk/>

Correlating three-dimensional morphology with function in PBDB-T:IT-M non-fullerene organic solar cells

Wei Li¹, Jinlong Cai¹, Yu Yan¹, Feilong Cai¹, Sunsun Li², Robert S. Gurney¹, Dan Liu¹, James D. McGettrick³, Trystan M. Watson³, Zhe Li⁴, Andrew J. Pearson⁵, David G. Lidzey⁶, Jianhui Hou², Tao Wang^{1*}

¹School of Materials Science and Engineering, Wuhan University of Technology, Wuhan 430070, China E-mail: twang@whut.edu.cn

²State Key Laboratory of Polymer Physics and Chemistry, Institute of Chemistry, Chinese Academy of Sciences

³SPECIFIC, College of Engineering, Bay Campus, Swansea University, Swansea, UK

⁴School of Engineering, Cardiff University, Cardiff, Wales UK, CF24 3AA

⁵Cavendish Laboratory, University of Cambridge, J. J. Thomson Avenue, Cambridge CB3 0HE, UK

⁶Department of Physics and Astronomy, University of Sheffield, Sheffield S3 7RH, UK

GISAXS modeling

To quantify and compare the phase separation in the non-fullerene photovoltaic blends, the 1D GISAXS profiles were fitted using a universal model expressed in Equation 1 using the fitting software SasView (Version 3.1.2). The first term of the equation is the so-called Debye–Anderson–Brumberger (DAB) term, where q is the scattering wave vector, A_1 is an independent fitting parameter, and ξ is the average correlation length of the PBDB-T domain. The second term represents the contribution from fractal-like aggregations of IT-M. Here, $P(q, R)$ is the form factor of IT-M. $S(q, R, \eta, D)$ is the fractal structure factor, which describes the interaction between primary particles (defined as 4 nm in our fitting) in this fractal-like aggregation system, with R the mean radius of primary IT-M aggregates, and η the correlation length of the fractal-like structure. The average correlation length of the clustered IT-M phases can be defined by the Guinier radius (R_g) of the network, where $R_g = \sqrt{\left(\frac{D(D+1)}{2}\right)}\eta$.

$$I(q) = \frac{A_1}{[1+(q\xi)^2]^2} + A_2 \langle P(q, R) \rangle S(q, R, \eta, D) + B \quad (1)$$

$$S(q) = 1 + \frac{\sin[(D-1) \tan^{-1}(q\eta)] b \pm \sqrt{b^2 - 4ac}}{(qR)^D} \frac{D\Gamma(D-1)}{\left[1 + \frac{1}{(q\eta)^2}\right]^{(D-1)/2}} \quad (2)$$

Calculation of donor:acceptor ratio from XPS measurements

XPS data were obtained using a Kratos Axis Supra (Kratos Analytical, Manchester, UK) having a monochromated Al K α source. All spectra were recorded using a charge neutralizer to limit differential charging. The main carbon peak is referenced to 284.5 eV. Depth profiles of different samples were generated by Minibeam 6 gas cluster ion source rastering a 2.5 kV Ar₅₀₀⁺ cluster beam over a 3 mm x 3 mm area giving a typical sample current of 5.53 nA. The data was fitted using CASA XPS with Shirley backgrounds using the Kratos sensitivity factor library. To identify PBDB-T and IT-M, we first measured the PBDB-T and IT-M pure films to identify the content of C, N, O, and S atoms in pure PBDB-T and IT-M films. Afterwards, we identify the C, S, O content in PBDB-T as C_{PBDB-T} wt%, S_{PBDB-T} wt%, O_{PBDB-T} wt%, and the C, S, O, N content in IT-M as C_{IT-M} wt%, S_{IT-M} wt%, O_{IT-M} wt%, N_{IT-M} wt%. We then measured PBDB-T:IT-M blend films and identified the C, N, O, S content as (C from blend) wt%, (N from blend) wt%, (O from blend) wt%, (S from blend) wt%. Since IT-M contain N atom but PBDB-T does not has N atom, we therefore use N atom to calculate the IT-M content in the PBDB-T:IT-M blend films. The content of C, O, S comes from IT-M can be calculated as:

$$(\text{C from IT-M}) \text{ wt}\% = (\text{N from blend film}) \text{ wt}\% * C_{\text{IT-M}} \text{ wt}\% / N_{\text{IT-M}} \text{ wt}\%,$$

$$(\text{O from IT-M}) \text{ wt}\% = (\text{N from blend film}) \text{ wt}\% * O_{\text{IT-M}} \text{ wt}\% / N_{\text{IT-M}} \text{ wt}\%,$$

$$(\text{S from IT-M}) \text{ wt}\% = (\text{N from blend film}) \text{ wt}\% * S_{\text{IT-M}} \text{ wt}\% / N_{\text{IT-M}} \text{ wt}\%.$$

Afterwards, we used (C from blend) wt%, (O from blend) wt%, (S from blend) wt% to deduce (C from IT-M) wt%, (O from IT-M) wt%, (S from IT-M) wt% to obtain the (C from PBDB-T) wt%, (O from PBDB-T) wt%, and (S from PBDB-T) wt%. Furthermore, we use (C from PBDB-T) wt%, (O from PBDB-T) wt%, (S from PBDB-T) wt% to check the accuracy of our results. The appearance of Ti atoms marks the appearance of the TiO₂ layer during depth profiling. The S atoms in PEDOT:PSS consist those from the thiophene unit in PEDOT and those from the sulfonate unit in PSS, whilst the S 2p of PEDOT and PSS locates at 165 and 169 eV respectively. The appearance of S atoms from the PSS unit marks the appearance of the PEDOT:PSS layer during depth profiling. As the ratio of S atoms from PEDOT and those from PSS is fixed, we can then determine the total S atoms contributed by PEDOT:PSS. Then the S atoms from PBDB-T can be obtained by subtracting the total S atoms by S atoms contributed by IT-M and PEDOT:PSS. All film thicknesses after etching were confirmed using a Dektak 150 stylus profilometer.

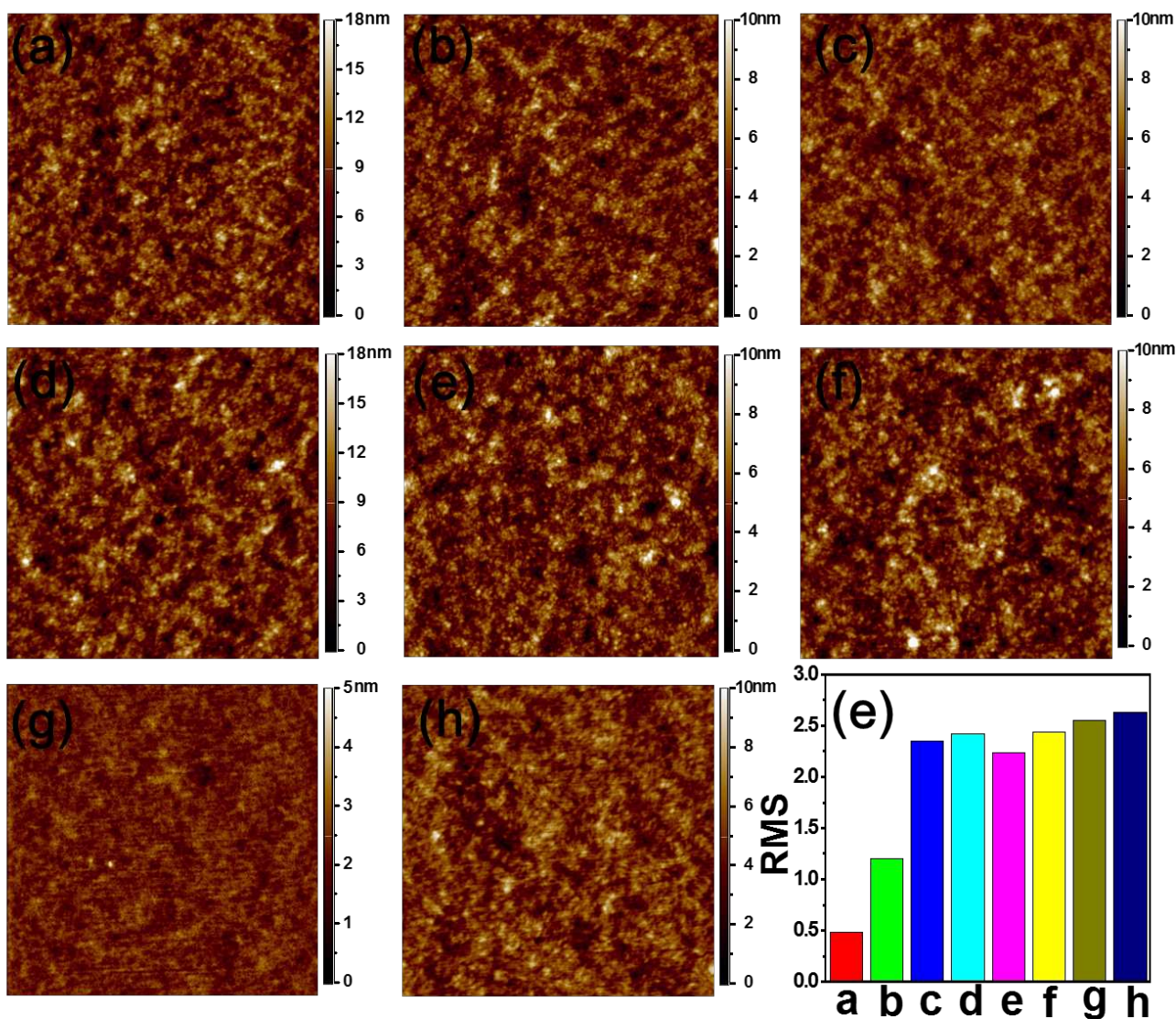


Figure S1 SPM topographic images of PBDB-T:IT-M films cast on (a, b, c) PEDOT:PSS and (d, e, f) TiO_2 substrates with (a, c) none annealing, (b, d) 80°C annealing, (c, f) 160°C annealing. (g) and (h) are SPM topographic images of pure PBDB-T and IT-M films. (e) The RMS surface roughness of images a-h.

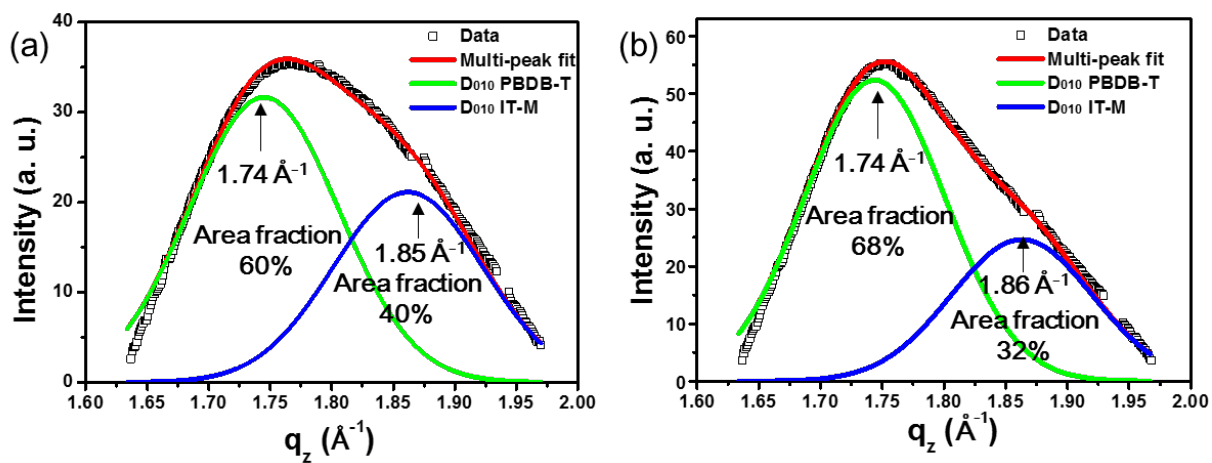


Figure S2. Multi-Peak fitting results of the OOP (010) peaks of PBDB-T:IT-M (a) upon 80 °C thermal annealing and (b) upon 160 °C thermal annealing.

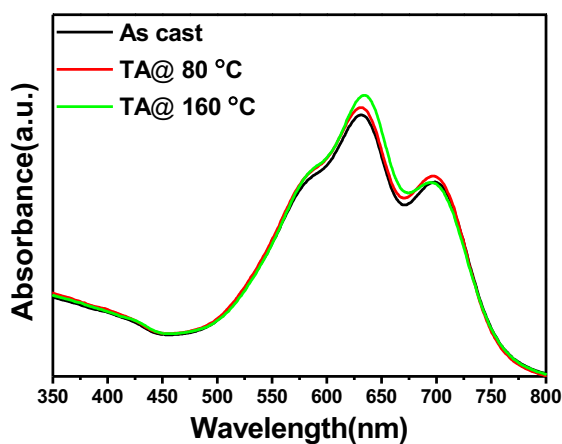


Figure S3. Absorption spectra of PBDB-T:IT-M with different annealing temperature.

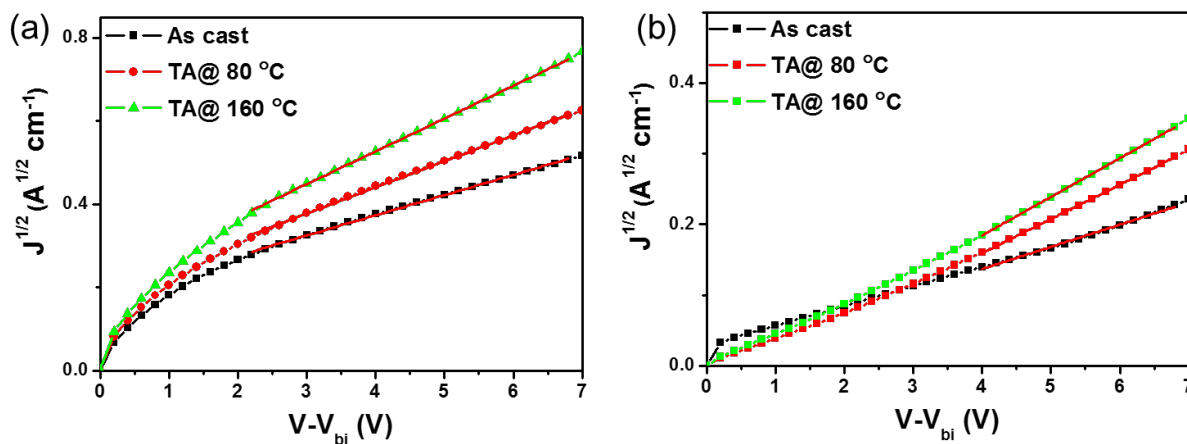


Figure S4. Root square plot of (a) electron current densities versus bias voltage of the ITO/TiO₂/Active layer/Ca/Ag electron-only devices after different annealing treatments, and (b) hole current densities versus bias voltage of the ITO/PEDOT:PSS/Active layer/MoO₃/Ag hole-only devices.

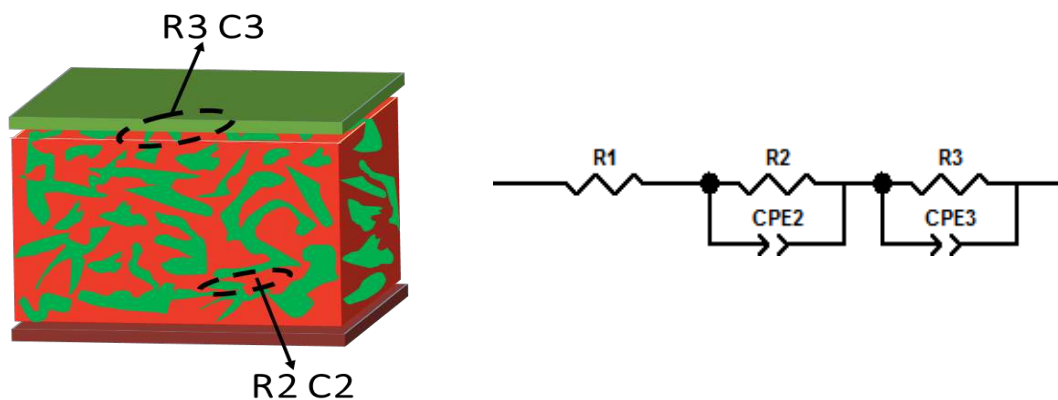


Figure S5. The equivalent circuit model to fit the impedance spectra.